

Article

Comparison of Raspberry Ketone Production via Submerged Fermentation in Different Bioreactors

Yi Zhang ¹, Eric Charles Peterson ^{2,*} , Yuen Ling Ng ³, Kheng-Lim Goh ³, Vladimir Zivkovic ⁴ and Yvonne Chow ^{5,*}

¹ Oil Crops Research Institute, Chinese Academy of Agricultural Sciences, Hubei Key Laboratory of Lipid Chemistry and Nutrition, Hubei Hongshan Laboratory, Key Laboratory of Oilseeds Processing, Ministry of Agriculture, Wuhan 430062, China; zhangyi07@caas.cn

² Centre Eau, Terre, Environnement (ETE), Institut National de la Recherche Scientifique (INRS), 490 Rue de la Couronne, Quebec City, QC G1K 9A9, Canada

³ Newcastle Research & Innovation Institute Singapore (NewRIIS), 80 Jurong East Street 21, #05-04, Singapore 609607, Singapore; yuenling.ng@newcastle.ac.uk (Y.L.N.); kheng-lim.goh@newcastle.ac.uk (K.-L.G.)

⁴ School of Engineering, Newcastle University, Newcastle Upon Tyne NE1 7RU, UK; vladimir.zivkovic@newcastle.ac.uk

⁵ Singapore Institute of Food and Biotechnology Innovation (SIFBI), Agency for Science, Technology and Research (A*STAR), Singapore 138669, Singapore

* Correspondence: eric.peterson@inrs.ca (E.C.P.); yvonne_chow@sifbi.a-star.edu.sg (Y.C.)

Abstract: Raspberry ketone (RK) has high commercial value in the food and healthcare industries. A biological route to this flavour compound is an attractive prospect, considering the need to meet consumer demands and sustainable goals; however, it is yet to become an industrial reality. In this work, fungal production of raspberry ketone (RK) and raspberry compounds (RC) via submerged fermentation of *Nidula niveo-tomentosa* was characterized in flask, stirred-tank reactor (STR), panel bioreactor (PBR), and fluidized bed reactor (FBR) configurations. The results indicate that the panel bioreactor resulted in larger, floccose pellets accompanied by maximum titres of 20.6 mg/L RK and 50.9 mg/L RC. The stirred-tank bioreactor with impeller mixing yielded compact elliptical pellets, induced the highest volumetric productivity of 2.0 mg L⁻¹ day⁻¹, and showed RK selectivity of 0.45. While differing mixing strategies had clear effects on pellet morphology, RK production presented a more direct positive relationship with cultivation conditions, and showed appropriate mixing and aeration favour RK to raspberry alcohol (RA). Overall, this paper highlights the importance of bioreactor design to fungal fermentation, and gives insight into green and industrial bioproduction of value-added natural compounds.

Keywords: raspberry ketone; fungal morphology; fermentation; bioreactor configurations; sustainable bioproduction



Citation: Zhang, Y.; Peterson, E.C.; Ng, Y.L.; Goh, K.-L.; Zivkovic, V.; Chow, Y. Comparison of Raspberry Ketone Production via Submerged Fermentation in Different Bioreactors. *Fermentation* **2023**, *9*, 546. <https://doi.org/10.3390/fermentation9060546>

Academic Editor: Xidong Ren

Received: 14 May 2023

Revised: 3 June 2023

Accepted: 5 June 2023

Published: 6 June 2023



Copyright: © 2023 by the authors. Licensee MDPI, Basel, Switzerland. This article is an open access article distributed under the terms and conditions of the Creative Commons Attribution (CC BY) license (<https://creativecommons.org/licenses/by/4.0/>).

1. Introduction

Bioproduction of natural and value-added compounds via cleaner pathways such as fermentation and enzymatic catalysis enables the sustainable, efficient, and purposeful production of desired chemicals [1,2]. For instance, 4-(4-hydroxyphenyl)-butan-2-one, commonly known as raspberry ketone (RK), is an important component of raspberry flavour that has been widely used in food and healthcare industries [3,4]. However, RK extraction from natural plants/fruits such as raspberries, blackberries, grapes and rhubarb is still limited by low yields (ranging from 1.1 to 4.2 mg/kg), although the price of natural RK can be as high as \$20,000/kg [5]. Meanwhile, chemical synthesis can effectively stimulate RK production, but associated issues such as high energy inputs, unexpected by-products and serious environmental threats limit our ability to meet the requirements of clean and carbon-negative production [6,7].

Recently, researchers have attempted to seek more sustainable sources of bioderived RK through microbial or enzymatic methods, which qualify as natural products according to the EC Flavour Directive [8]. For instance, Andreas Boker, et al. [9] used the basidiomycete *Nidula niveo-tomentosa* to demonstrate a maximum yield of 200 mg/L of raspberry compounds (the mixture of RK and its alcohol by-product) in optimized media with supplied aromatic precursors of L-phenylalanine or L-tyrosine. Similarly, microbial production of natural RK from p-coumaric acid in heterologous systems such as *Escherichia coli* (5 mg/L) and *Saccharomyces cerevisiae* (trace amounts) has also been demonstrated [10]. To date, RK bioproduction has typically been reported in small flask-scale submerged cell cultivation, where mass transfer and dissolved oxygen are expected to be limited, and this affects cell growth and process performance. Additionally, raspberry ketone has been observed to be subsequently transformed into Raspberry Alcohol (RA), which was confirmed by Zorn et al. [11], who used labelling studies of ^{13}C -labeled L-phenylalanine and [$1\text{-}^{13}\text{C}$] glucose to detect the biotransformation from RK into RA in submerged cultivation of *Nidula niveo-tomentosa*. If optimal production is going to be achieved in terms of RK production, an understanding of the relationship between cultivation conditions and process performance would be beneficial. For industrial applications, standard reactors are available for bacteria and yeast, whereas for fungal bioprocesses, no ideal bioreactor designs have been established for routine industry production [12,13]. Therefore, there is a need to determine an appropriate bioreactor design for scaling up to an industrial bioprocess.

Bioreactor systems such as stirred-tank reactors (STR), photobioreactors, airlift bioreactors, and fluidized bed reactors (FBR) have also been used widely for bioprocessing and bioproduction [14,15]. Unlike flask cultivation, bioreactor systems enable improved bioprocess control via agitation and/or aeration, thus achieving constant cultivation conditions and promoting biological production. For instance, in a stirred-tank reactor, increasing agitation minimizes the formation of the product's concentration gradient [16,17], but the associated intensive mechanical stirring can induce high shear stress, which could result in adverse effects on the microorganisms, especially if they are shear-sensitive [18]. Airlift bioreactors and fluidized bed reactors can bring about mixing and mass transfer while avoiding mechanical stress, and are commonly used for aerobic cultivation conditions. However, the control of mixing using upward bubble movement leads to sedimentation or wash-out when the aeration rate is too low or too high, respectively [19,20]. Regardless, different agitation and aeration systems (i.e., mechanical agitation vs. airlift) have strong effects on fungal morphology (i.e., mycelia vs. pellet vs. clump formation). For instance, Taymaz-Nikerel et al. confirmed that aeration encouraged floccose pellet formation, but the higher agitation led to dense pellets with a compact pellet surface [21]. Similarly, the effect of agitation intensity on pellet morphology was also reported by Porcel et al. [22], who demonstrated that the diameter of *Aspergillus terreus* pellets decreased from 2300 μm to less than 900 μm when the agitation intensity increased from 300 rpm to more than 600 rpm in a stirred-tank fermenter. These changes in morphology can subsequently influence the fermentation performance and the related productivity [23]. However, the evidence on the impact of agitation intensity on total fungal biomass provided in the literature is debatable. Porcel et al. [22] demonstrated a biomass yield of 2 g/L for *Aspergillus terreus* regardless of the agitation speed (i.e., 300, to 600 and 800 rpm), suggesting that mixing had no effect on this response variable. In contrast, Amanullah et al. [24] argued that the biomass concentration increased with increasing agitation intensity in fed-batch cultures of *Aspergillus oryzae*, as hyphal shearing from the pellet surface allows subsequent fragments to reseed, forming new pellets [25]. Alternatively, it is possible that the differences observed from these studies could be due to the aeration changes, as high levels of dissolved oxygen have been widely acknowledged to lead to a high biomass concentration [26,27].

An understanding of the relationship between pellet morphology and bioprocess performance for a given fungal strain and target bioproduct is fundamentally important, especially for sustainable, high-efficiency and high-selectivity industrial production. In this

paper, the impact of various reactor designs with different modes of mixing and aeration on RK production with *Nidula niveo-tomentosa* is determined. Fermentations were performed on three different bench-scale fermenters, namely a stirred-tank reactor (STR, 750 mL), a panel bioreactor (PBR, 400 mL), and a fluidized bed reactor (FBR, 1L), and compared to flask culture controls (48 mL). Understanding the relationship between reactor design, fungal morphology, and subsequent metabolite production will be of fundamental importance for improved RK production and the scaling up of sustainable production in future.

2. Material and Methods

2.1. Chemicals

The substrates for culture media were purchased from Sigma-Aldrich (Singapore), Merck (Darmstadt, Germany), Kento (Tokyo, Japan), 1st BASE (Gemini, Singapore), and BD (Miami, FL, USA). HPLC calibration standards, including RK, rhododendrol and L-phenylalanine, were purchased from Sigma-Aldrich (Shanghai, China). Solvents were purchased from VWR (Paris, France) and 1st BASE (Gemini, Singapore).

2.2. Microorganism and Cultivation

The *Nidula niveo-tomentosa* strain (CBS strain 380.80) was provided courtesy of the Zorn group from Leibniz University Hannover [28]. For long-term storage and preservation, culture stocks of the strains were kept at $-70\text{ }^{\circ}\text{C}$ with 15% (*v/v*) glycerol in 1 mL aliquots. Seed culture was prepared by adding one aliquot of thawed stock culture into 40 mL of culture medium. The culture medium contained 75 g/L glucose monohydrate, 6 g/L soy peptone, 1.5 g/L yeast extract, 2.5 g/L KH_2SO_4 , 0.5 g/L MgSO_4 , 73.5 mg/L $\text{CaCl}_2 \cdot \text{H}_2\text{O}$. The seed culture was grown aerobically in 100 mL Erlenmeyer flasks in a MaxQ™ 6000 shaking incubator (ThermoFisher Scientific, Waltham, MA, USA) at 150 rpm and $24\text{ }^{\circ}\text{C}$. The cultivation period of seed culture was 14 days for fungi proliferation and pelletization, after which the seed culture was homogenized aseptically at a speed of 10,000 rpm for 1 min using a T18 digital ULTRA-TURRAX® homogenizer (IKA, Staufen, Germany). The homogenized seed culture was then used for fungal inoculum. The homogenate inoculum was then added to flasks containing sterile culture media.

2.3. Experimental Design

To stimulate RK production, 10% (*v/v*) of filter sterilized phenylalanine (110 mM) was added to the fungi culture medium, and the cultures were irradiated using UV-A light with a photoperiod of 10 h UV light and 14 h dark. The blacklight UV tubes (F4T5BLB 352 mm \times 6, SANKYO DENKI, Hiratsuka, Japan) were mounted on the top face of incubator for flask controls, or in a UV enclosure for bioreactors.

2.4. Flask Culture

The fungi culture medium consisted of 40 mL fresh medium, 4 mL of 110 mM phenylalanine and 4 mL of homogenized seed culture in a 100 mL Erlenmeyer flask. The flask's culture was then cultivated in a MaxQ™ 6000 shaking incubator (ThermoFisher Scientific, USA) with a rotational speed of 150 rpm at $24\text{ }^{\circ}\text{C}$ for 5 weeks.

2.5. Stirred-Tank Reactor

A lab-scale stirred-tank reactor (Sartorius Stedim, Guxhagen, Germany) of 1 L capacity was used, with a working volume of 750 mL of fungi culture medium (625 mL of fresh medium + 62.5 mL of 110 mM phenylalanine and 62.5 mL of homogenized seed culture), at $25\text{ }^{\circ}\text{C}$. The agitation speed and aeration flowrate were maintained at 300 rpm and 0.15 v.v.m, respectively, while the pH of the bioreactor was not controlled but monitored using the inline system.

2.6. Panel Bioreactor

Fungal fermentation using a panel bioreactor (PBR) was carried out in an FMT 150/400 flat-panel photobioreactor (PSI Photon system Instruments, Drasov, Czech Republic), in which 400 mL of fungi culture medium was cultivated (Figure 1a), with aeration provided at a fixed gas flowrate of 0.15 v.v.m. and delivered via tubing (\varnothing 6/3 mm) through two headplate Luer connectors to reach a bottom-mounted stainless-steel U-tube sparger with aeration holes (\varnothing 1 mm). To facilitate mixing, as an option, a magnetic stirrer with 35 mm long (\varnothing 6 mm) teflon-coated magnets controlled by the computer-controlled monitoring device could be used to promote mixing and minimize the dead zone. Similarly, the PBR was also irradiated using the same UV-A light for 10 h daily during the fermentation period.

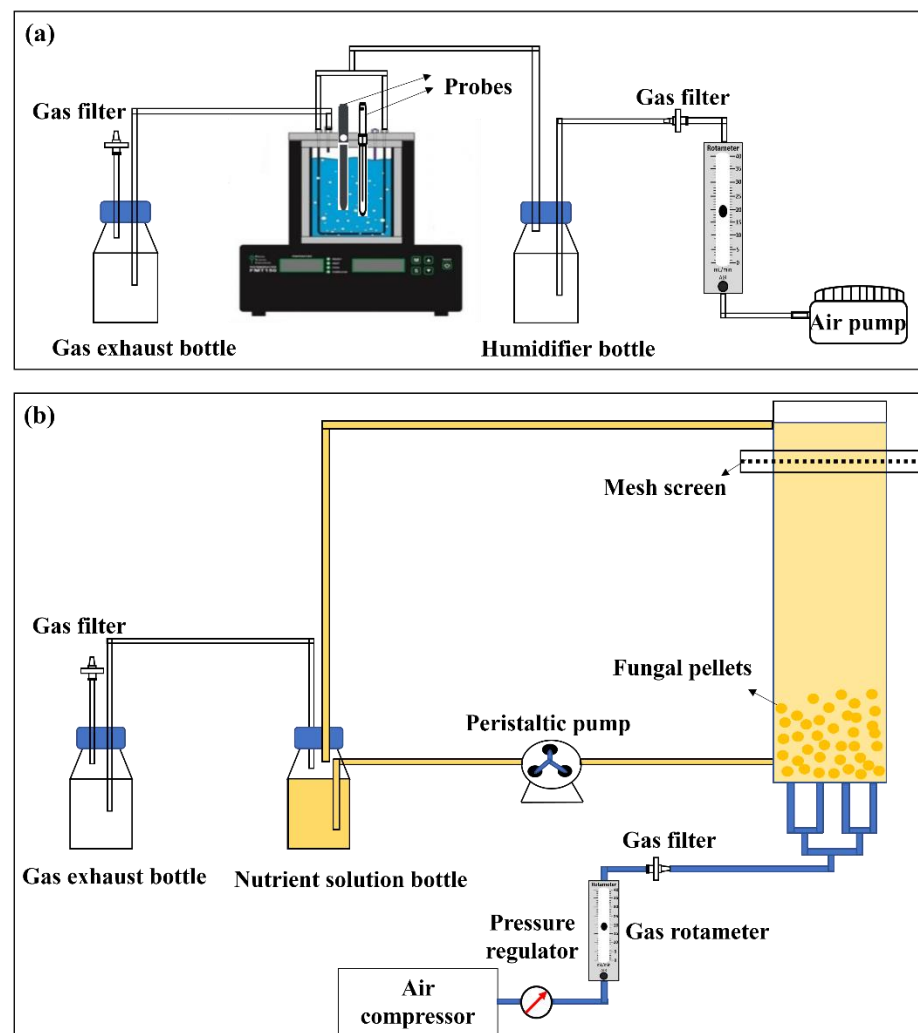


Figure 1. Schematic diagrams of the experimental setup: (a) panel bioreactor (PBR), (b) fluidized bed reactor (FBR).

2.7. Fluidized Bed Reactor

The schematic diagram of the experimental setup for liquid–solid and liquid–gas–solid fluidization system (1 L in total volume) is shown in Figure 1b. This lab-scale fluidized bed reactor (FBR) comprised two sections: (a) a lower section, including liquid inlets on two sides, four base-mounted gas spargers (\varnothing 150 μ m \times 4) and a main column (5 \times 5 cm in cross section, 20 cm in height); and (b) an upper head plate (5 \times 5 cm in cross section, 5 cm in height) containing the gas/liquid outlet. The two sections were made of 3 mm thick quartz plates (Qudao Quartz Ltd., Lianyungang, China), and connected via flat flange plates. Each plate is fitted with an O-ring rubber gasket (to prevent liquid/gas leakage).

Between the two flange plates, a stainless-steel mesh screen (40 μm mesh size) was inserted to prevent pellet washout during liquid discharge for pellet fluidization. Gas sparging is carried out through four gas inlets ports at the base, with glass capillary tubing (CM Scientific, Keighley, UK) of 3 mm and 150 μm outer and inner diameter, respectively. For the purpose of consistent comparison, an air supply rate of 0.15 v.v.m was employed. A more detailed summary showing the main operating conditions in the flask, STR, PBR, and FBR is listed in Table 1.

Table 1. Summary of the main operating parameters in different bioreactor systems.

| Operating Conditions | Flask | STR | PBR | FBR |
|-------------------------|-------|------|-------|-------|
| Cultivation volume (mL) | 48 | 750 | 400 | 1000 |
| Aeration rate (v.v.m) | / | 0.15 | 0.15 | 0.15 |
| Liquid flowrate (mL/s) | / | / | / | ~0.25 |
| Agitation rate (rpm) | / | 300 | 0–180 | / |
| UV-A radiation (h/day) | 10 | 10 | 10 | 10 |

2.8. HPLC and YSI Analysis

The RK, RA, and phenylalanine concentrations were detected via high-performance liquid chromatography (HPLC), and then quantitatively calculated based on the calibration curves. Briefly, mobile phase A was 0.1 M sodium acetate buffer, whose pH was adjusted to 4.66 by acetic acid, while mobile phase B was pure methanol. The analysis involved an Agilent 1260 Infinity LC System equipped with a ZORBAX, Eclipse Plus C18, 4.6 \times 50 mm², 5 μm column. For each sample, filtered culture media were injected into the C18 column (Agilent Technologies, Santa Clara, CA, USA), and conditions were as follows: injection volume, 20 μL ; mobile phase flow rate, 0.5 mL/min; column temperature: 35 $^{\circ}\text{C}$. A gradient method comprising 0.1 M sodium acetate buffer (mobile phase A) and pure methanol (mobile phase B) was applied as follows: 0–2.5 min 75% A/25% B, 2.5–9 min 60% A/40% B. The detection wavelength for RK and RA is 280 nm, and for phenylalanine is 290 nm. The RK/RA concentrations were determined from calibration curves obtained with commercial standards.

Glucose concentrations in culture media during the fungal fermentation were measured using a YSI 2900 Analyzer (Yellow Springs Instrument Inc, Yellow Springs, OH, USA), which reflected the glucose consumption by comparing the initial and real-time glucose concentrations in different fermentation periods. As the maximum glucose concentration in YSI 2900 that can be detected is 25 g/L, all the liquid samples were diluted with ultrapure water ten times before glucose concentration measurements. Therefore, it should be noted that the actual glucose concentration of liquid samples should be ten times larger than the values displayed on the YSI screen.

2.9. Other Characterizations

2.9.1. Biomass Determination

The final biomass, expressed as the dry weight (g/L) of fungal pellets, was obtained by filtering the contents of the flask/reactor through a pre-weighed filter paper with a Buchner funnel, thereafter drying the filter paper with the residue in a 55 $^{\circ}\text{C}$ drying oven (Binder FD 240, Germany) for 24 h. The weight of the dried residue was regarded as the pellet dry weight.

2.9.2. Pellet Morphology

After the fermentation, pellet samples were collected from different bioreactors and subsequently transferred from the flask into Petri dishes for photographic image acquisition using a Scan 1200 (Interscience, Saint-Nom-la-Bretèche, France) colony counter. Pellet size and sphericity were measured using the Analyze-Particles function in ImageJ software [19,29].

3. Results and Discussion

3.1. Pellet Morphology and Biomass Distribution

To determine how the growth and morphology of filamentous fungi in submerged cultures is influenced by the bioreactor design and corresponding operating conditions, pellet morphologies of *Nidula niveo-tomentosa* were characterized during the 4-week fermentation in flask, STR, PBR, and FBR. As shown in Figure 2a, fungi species in flasks grew into compact pellets surrounded by hyphae, which exhibited the smallest size (2.27 ± 0.48 mm) but the highest sphericity (0.88 ± 0.06) compared to those grown in STR, PBR, and FBR. Interestingly, while the fungal pellets in the STR (Figure 2b) were also compact pellets similar to flask culture, they showed an elliptical nature, (3.16 ± 1.80 mm in diameter, 0.62 ± 0.17 mm in sphericity), and lacked a hyphal fringe. Thus, impeller-based agitation (300 rpm) of the STR had more impact on pellet sphericity than the pellets' size. Figure 2c,d indicate the pellets' morphologies in PBR and FBR, respectively. Both PBR and FBR had a gas flowrate of 0.15 v.v.m to suspend the pellets, but the main difference between PBR and FBR was the involvement of the magnetic stirrer in PBR, which mitigated the dead zone and improved mass transfer. However, mechanical stress from the magnetic stirrer could induce the pellets' breakage, which was not observed in the FBR due to the absence of mechanical stirring.

As a result, the FBR showed a noticeable increase in pellet diameter (7.49 ± 1.83 mm) and sphericity (0.83 ± 0.08) compared to the pellets in PBR (4.43 ± 1.35 mm in diameter, 0.75 ± 0.10 in sphericity (Figure 2c–e). Enlargement of pellet morphology as a result of continuous gas flow in FBR designs has also been reported by Moreira et al. [30], who compared the effects of a pulsed flow and a non-pulsed system on fungal pellet morphology, confirming that a fluidized bed bioreactor without pulse treatments led to bigger pellet sizes for *Aspergillus niger* and *Phanerochaete chrysosporium*. Therefore, in using improved upward flow and minimal bubble disturbance, the FBR represents an improved design compared to the PBR, overcoming the need for magnetic stirring while avoiding bubble rupture disturbance, thereby maintaining pellet integrity.

Despite differences in morphology, the total biomass was surprisingly unchanged regardless of the cultivation system. As can be seen in Figure 2f, after 4 weeks of fermentation, the culture final dry weight reached 13.5 ± 1.0 , 13.4 ± 0.2 , 14.6 ± 0.5 and 13.3 ± 0.1 g/L in the flask culture, STR, PBR, and FBR, respectively, suggesting that under mixing conditions of 300 rpm agitation speed or 0.15 v.v.m gas flowrate, no comparable differences can be observed in the final obtainable biomass growth. This consistency in final biomass yields suggests that there was no limitation on growth in terms of dissolved oxygen or substrate availability. A more comprehensive study on fungal biomass growth rate is needed to confirm the relationship between fungal biomass and dissolved oxygen. In this work, it can be seen that fungal pellet morphology differs substantially between gas-mixed and impeller-agitated systems. As summarized in Figure 2g, gas mixing gives rise to expanded, low-density floccose pellets, in comparison to dense smooth pellets under mechanical mixing; however, these differences do not have any impact on the attainable biomass concentration.

3.2. Production of Raspberry Compounds and Glucose Uptake

While no difference was observed in total biomass across the systems tested, pellet morphology varied substantially according to bioreactor design, and thus the relationship between RK production, bioreactor conditions, and pellet morphology was investigated. As shown in Figure 3a, RK in flask, STR, and FBR reached maximum values of 13.7 ± 1.2 mg/L, 18.9 ± 0.7 mg/L and 7.4 ± 0.1 mg/L at week 2.5, week 3 and week 2.5, respectively, while RK in PBR kept increasing to a highest point of 20.6 ± 0.7 mg/L by the end of a 4-week fermentation. Notably, the poor RK in FBR was mainly due to the aeration rate of 0.15 v.v.m, which was insufficient to suspend the growing pellets. Importantly, as RK is subsequently converted to raspberry alcohol (RA) by a subsequent reduction, the RA in all bioreactors was observed to continually increase during the fermentation [11], as shown in Figure 3b.

Thus, the sum of these two raspberry compounds (RC) can be considered an indication of the metabolite production level, giving insight into the overall fermentation (Figure 3c). Similarly to RK production, the highest RC titre of 50.9 ± 2.8 mg/L was also achieved in the PBR, followed by the STR (RC = 41.5 ± 1.5 mg/L), flask (RC = 38.3 ± 1.2 mg/L), and FBR (RC = 20.2 ± 1.9 mg/L).

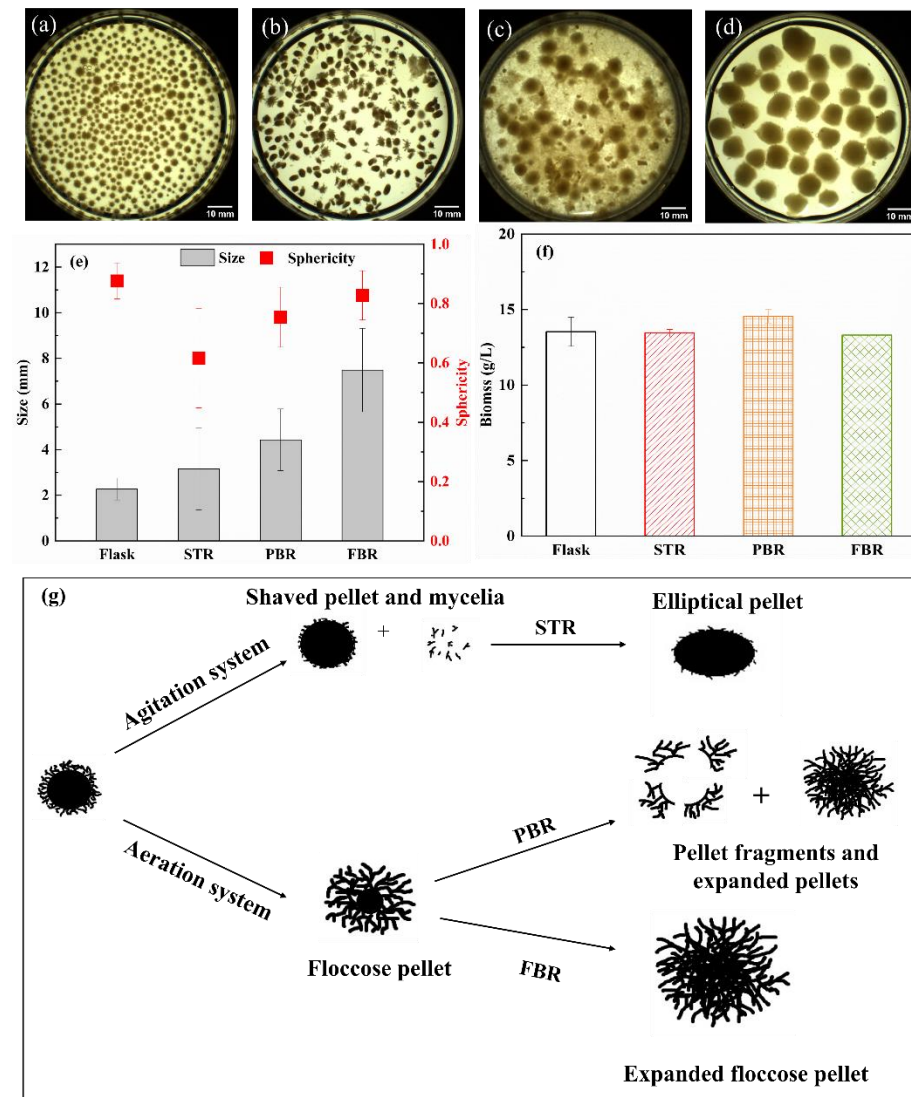


Figure 2. Images of pellet samples after 5-week fermentations in (a) flask culture, (b) STR, (c) PBR, and (d) FBR. (e) Pellet size and sphericity after 5-week fermentation in different bioreactors, (f) Biomass concentrations of fungal cells after 5-week fermentation in different bioreactors and (g) Illustration of the pellet’s morphology variation in different bioreactors.

Based on the summary of the titre concentration, yields, and productivities of these compounds shown in Table 2, it should be noted that the maximum values for each treatment for both RK and RC were achieved simultaneously. The time taken to reach these values (i.e., peak production point for RK) varied with the culture vessel used, wherein the flask experiments and FBR reached an endpoint after 2.5 weeks, while the STR stabilized at 3 weeks, and the PBR showed steady production over the entire 4 weeks. Importantly, the highest volumetric productivity for RK, as calculated by the peak production point, was achieved in the STR ($0.90 \text{ mg L}^{-1} \text{ day}^{-1}$), followed by flask ($0.78 \text{ mg L}^{-1} \text{ day}^{-1}$), PBR ($0.74 \text{ mg L}^{-1} \text{ day}^{-1}$), and FBR ($0.42 \text{ mg L}^{-1} \text{ day}^{-1}$). Thus, STR showed the best rates of production in the systems studied here.

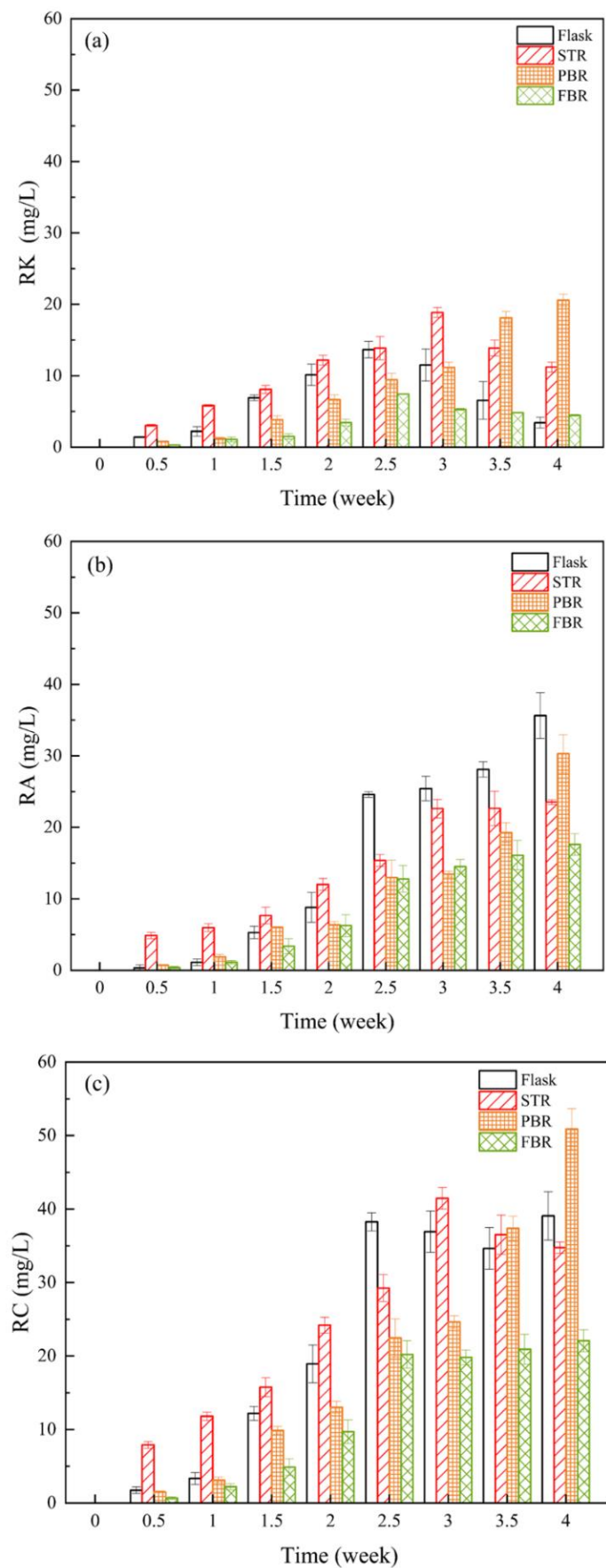


Figure 3. Bioproduction in different bioreactors over 4 weeks of fungal fermentation: (a) RK production versus time, (b) RA conversion versus time, (c) total RC concentration versus time.

Table 2. Various yield values at peak production points in different bioreactors, using glucose and phenylalanine as substrate.

| Yields | Flask | STR | PBR | FBR |
|-------------------------------------|-------------|-------------|-------------|-------------|
| Peak production point (week) | 2.5 | 3.0 | 4.0 | 2.5 |
| RK (mg/L) | 13.7 ± 1.2 | 18.9 ± 0.7 | 20.6 ± 0.7 | 7.4 ± 0.1 |
| RA (mg/L) | 24.6 ± 0.4 | 22.6 ± 1.3 | 30.3 ± 2.7 | 12.8 ± 1.9 |
| RC (mg/L) | 38.3 ± 1.2 | 41.5 ± 1.5 | 50.9 ± 2.8 | 20.2 ± 1.9 |
| RC $Y_{P/S}$ of glucose (mg/g) | 7.1 ± 0.5 | 3.8 ± 0.2 | 2.5 ± 0.9 | 1.3 ± 0.1 |
| RC $Y_{P/S}$ of phenylalanine (g/g) | 52.1 ± 0.1 | 68.1 ± 0.2 | 54.2 ± 2.8 | 49.8 ± 0.1 |
| RK Vol. prod.* | 0.78 | 0.90 | 0.74 | 0.42 |
| RC Vol. prod.* | 2.19 | 1.97 | 1.82 | 1.16 |
| RK selectivity | 0.36 ± 0.09 | 0.45 ± 0.05 | 0.40 ± 0.07 | 0.37 ± 0.09 |

* Vol. productivity (mg L⁻¹ day⁻¹).

The RK selectivity, defined by the fraction of RK product over total product (RC), in different bioreactors is shown in Figure 4. Similar to productivity, STR shows the strongest selectivity for RK at the peak point (i.e., 0.45), followed by PBR (i.e., 0.40), with both the flask and FBR showing a selectivity of 0.36. As both dense pellets (i.e., flask) and floccose pellets (i.e., FBR) showed equal proportions of RK and RA, this suggests RK selectivity is independent of pellet morphology and relies on more reactor conditions, whether these be dissolved oxygen levels or improved mass transfer via mixing. It is possible that STR showed better selectivity because the small compact pellets facilitated effective dissolved oxygen delivery, and efficient mixing by agitated impellers minimized the formation of a product concentration gradient, while PBR also enjoyed effectively aerated conditions [16,17]. Conversely, the lower selectivity caused by the collapsed bed of FBR helps to illustrate the link between lack of appropriate aeration, mixing, and increased RA accumulation.

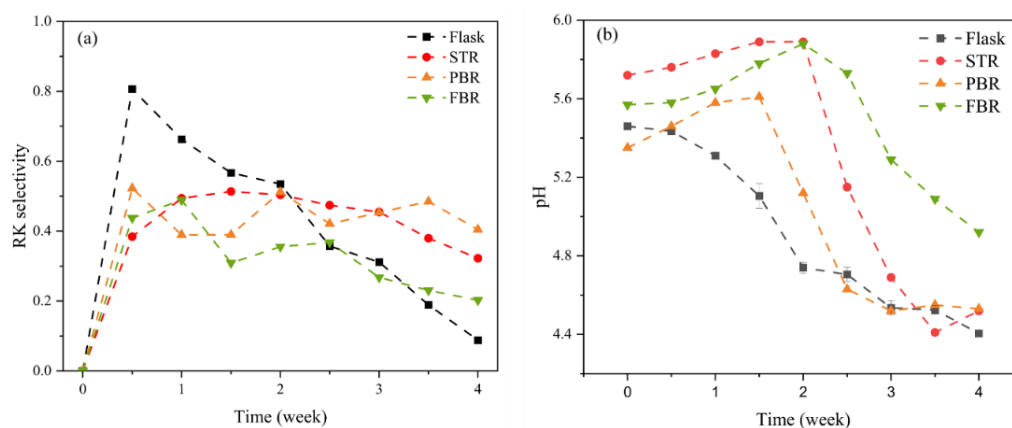


Figure 4. (a) Selectivity of RK versus time, (b) pH profile in different bioreactor systems during fungal fermentation.

As illustrated in Figure S1, phenylalanine used as the precursor could help the synthesis of RK, which was subsequently converted into RA due to the potential reductive hydrogenation in acid conditions, reflected by the pH profile in Figure 4b. The detailed phenylalanine consumption curves in different bioreactors during the fungal fermentation is shown in Table S1, which can also be used to explain the RK concentration change (Figure 4a), as well as the different RK selectivity in Table 2.

It can be observed that in the flask culture study, the proportion of RK sharply increases, followed by a strong constant decline, with the strongest transition to RA observed in this study, as evidenced by selectivity (i.e., 0.35). Conversely, both the STR and PBR did not show a rapid transition from raspberry ketone to raspberry alcohol, showing relatively stable values after an initial rise, and this may be due to relatively improved oxygenation

as well as improved mass transfer when compared to that in the flask and FBR. Regardless of pellet morphology, a combination of mixing and aeration had positive effects on RK selectivity. It is also interesting to note that the glucose concentration profiles in Table S2 reveal that more glucose was consumed by the floccose pellets in the FBR and PBR compared to the compact pellets in flasks and STR. Conversely, while the flask treatment showed a low titre and selectivity, it provided the highest glucose to product yield ($Y_{P/S}$) of 7.1 mg/g. In all treatments, glucose consumption was steady, and often continued past endpoint. This confirms that glucose consumption is not correlated with the production of this secondary metabolite. Comparatively, RK yields with respect to phenylalanine consumption (Table 2) show that conversion was the most optimal for the STR, adding further evidence that the combination of strong mixing and aeration were beneficial for RK production.

3.3. Bioreactor Mixing Characteristics

As demonstrated above, different reactors with certain agitation and aeration designs have clear effects on pellet morphology, and these changes in morphology in turn affect reactor performance. It is interesting to note that STR pellets were small and compact, and showed better productivity ($0.9 \text{ mg L}^{-1} \text{ day}^{-1}$) than the PBR treatment ($0.73 \text{ mg L}^{-1} \text{ day}^{-1}$) which led to larger expanded pellets. Thus, it could be that more vigorous mixing, for example, in the flask culture and STR, promotes greater rates of production (which could be a direct impact of mixing) or the formation of smaller pellets, both of which could increase mass transfer. It may be equally possible that these smaller pellets and more rapid mixing allow for greater exposure of the fungus to UV light bombardment, which is a requisite for RK formation.

For a fair comparison, a fixed aeration rate of 0.15 v.v.m was maintained across each reactor design. The PBR required additional magnetic stirring to avoid severe dead zone formation; this caused pellet breakage and more turbid conditions (Figure 2c). Conversely, the FBR approach generates large, unbroken pellets, showing a substantially different pellet morphology from both the flask and STR. The FBR is mixed using bubbling alone, and as a result, the aeration rate of 0.15 v.v.m employed in this study was not sufficient to suspend the pellets throughout the entire culture period. As shown in Figure S2, fungal pellets were observed to be fully fluidized and homogeneously suspended by the bubble flows in the first two weeks, during which time the inoculated seed culture grew into pellets. From week 3, as pellets became enlarged and more hirsute, this led to insufficient upward flow from aeration, resulting in partial pellet agglomeration and sedimentation, with some pellets remaining in suspension. By week 4, all the pellets were settled on the bottom of column, forming a packed bed likely to be limited in air supply. The diminished circulation and air availability under the partially fluidized bed and packed bed regimes from week 3 to week 4 caused RC production to stop, and RK concentration to decrease. The poor mass and oxygen transfer may have promoted the conversion of RK to RA, as implied by the respective concentration trend in Figure 4. It would be possible to overcome this pellet agglomeration with dynamic aeration, however, and to achieve better results in the FBR.

Thus, different gas flowrates of 0.15, 0.3 and 0.45 v.v.m were studied regarding their effects on fungal growth and RK production. As shown in Figure 5a, the final biomass dry weight increased from 13.3 g/L to 18.1 and 14.8 g/L, when the gas flowrate increased from 0.15 v.v.m to 0.30 and 0.45 v.v.m, respectively. The lowest biomass growth in the experiments with a 0.15 v.v.m gas flowrate was because of the early pellet sedimentation due to the insufficient gas flow. However, the biomass in the experiments with the 0.45 v.v.m gas flowrate was lower than that with 0.30 v.v.m, indicating that the much higher gas flow might cause strong shear stress on pellet growth, as a higher gas flowrate led to more breakage of pellets into fragments. The curves of RK production are presented in Figure 5b, in which the RK concentration increased from 0 in week 0 to the maximum point at around week 2 before their reductions. Specifically, the highest RK concentration

of 11.5 mg/L was achieved with a corresponding gas flowrate of 0.3 v.v.m, because both the early pellet sedimentation at a lower gas flowrate (0.15 v.v.m) and the severe pellet elutriation at a higher gas flowrate (0.45 v.v.m) inhibited the bioproduction. However, the final RK concentrations were relatively close, as RK was rapidly consumed due to the poor mixing and oxygen supply in the packed bed regime, occurring in all the cases in the final week of the experiments. The low mass transfer and poor gas supply led to the accumulation of RA, as oxygen is believed to delay the RK–RA conversion. In other words, poor gas supply will result in a greater RK reduction but a high RA accumulation. This is confirmed by Figure 5c, which shows that the highest RA concentration was from the condition with the lowest gas flowrate of 0.15 v.v.m. A slight reduction in RA was noted for the conditions of 0.30 and 0.45 v.v.m at the end of fermentation, indicating that other bioconversions involving RK and/or RA conversions took place at relatively higher gas flowrates, leading to higher compound accumulation in 0.15 v.v.m than that in higher gas flowrate conditions (Figure 5d). In summary, a fixed gas flowrate ranging from 0.15 to 0.45 v.v.m with 0.15 mm gas sparger ID cannot provide the complete pellet fluidization within the 4-week fermentation, due to the small bubble size and increased pellet biomass. The optimal gas flowrate of 0.30 v.v.m not only showed higher mass transfer and gas supply compared to 0.15 v.v.m gas flow, but also mitigated pellet elutriation compared to higher gas flowrates, thus leading to higher biomass accumulation and RK synthesis.

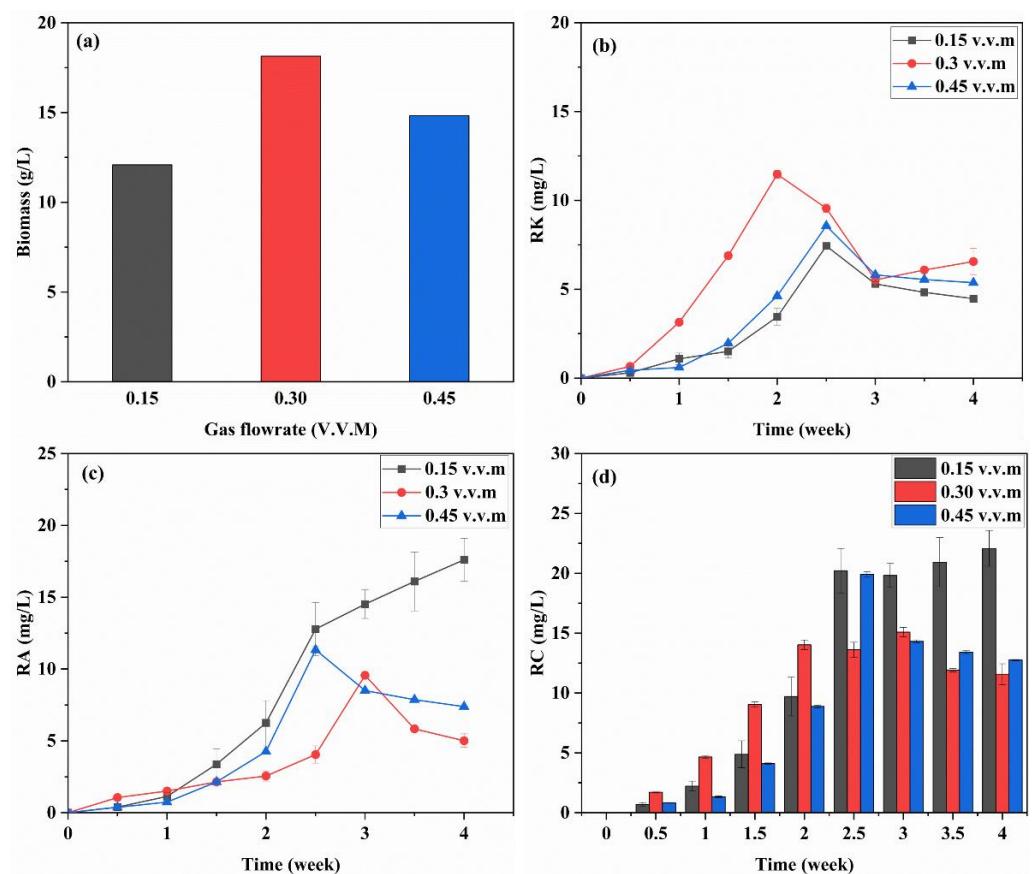


Figure 5. Study of gas flowrates on fungal growth and bioproduction: (a) final biomass dry weights under different gas flowrates, (b) RK curves during 4-week fermentation, (c) RA production during fermentation, and (d) RC accumulation during the fermentation.

3.4. Challenges and Prospects of Different Bioreactor Designs

To date, RK production using *Nidula niveo-tomentosa* reported in the literature has mainly been conducted in flask culture. The present study sheds light on the comparative effects of different bioreactor systems on fungal morphology, which is linked to bioproduc-

tion. The results indicate that a filamentous morphology is more appropriate for long-term fermentation, as the fungal fragments in PBR resulted in a continual increase in RK over the 4 weeks of fermentation; meanwhile, RK production in the flask and STR systems rapidly accumulated faster, thus saving fermentation time, which could have significant ramifications for capital and operational costs. Care must also be taken to maintain conditions that favour RK selectivity (i.e., well-mixed aeration systems). It should also be noted, however, that excessive growth of free mycelia represents operational problems. For instance, mycelia were observed to aggregate and attach to the baffles of STR, and to form dead zones in the vessel corners of the PBR. Other issues such as fouling of the fermenter probes, back growth along nutrient feed and sampling lines, losses in efficiency due to increased viscosity, and limited mass transfer have also been reported by other researchers [30,31].

One advantage of the fluidized bed reactor is that it can provide mixing without additional hardware such as a shaking bed or impellers. Similar to batch cultivation in a flask, the design of the STR and PBR facilitates intensive mixing in a manner similar to a shaking bed with impellers, or aeration-based mixing systems. Conversely, a fluidized bed reactor relies on continuous upflow, which not only enables mixing, but also the circulation of nutrients and metabolites. However, care must be taken to avoid overly strong upflow, which can cause pellet elutriation and biomass loss. On the other hand, an insufficient upflow in an FBR could result in pellet agglomeration and sedimentation, which mitigates the bioproduction of RK, as reported here. In recent years, many researchers have also reported the application of fluidized bed reactors in bioproduction and bioprocessing. For instance, Pereiro et al. [32] used a magnetic fluidized bed to capture and detect infectious bacteria. Silva et al. [33] investigated hydrogen production using anaerobic fluidized-bed reactors, and reported that the best values of hydrogen production were achieved with the system operating at minimum fluidization velocity (1.24 cm/s). These reports were based on the fluidization of solids prepared from surface functionalized beads [32,34,35] or immobilized cells/enzymes [33,36], which had very stable solid sizes and could maintain homogenous fluidization with a fixed liquid/gas flowrate, leading to good bioproduction performance. However, in the fungal fermentation study presented here, although fungal pellets could be directly fluidized using bubble flows, without the need for surface functionalization or solid immobilization, the pellet size continued to increase and the pellet morphology became floccose during the fermentation, which means a fixed gas flowrate was unable to maintain pellet fluidization. Thus, the decrease in RK from the third week of fermentation in the FBR design reported here can be attributed to pellet settlement due to an insufficient gas flowrate (0.15 v.v.m), which could only maintain the fluidized bed in the first 2 weeks of fermentation. With continual pellet size increase and biomass growth, it gradually turned into a partially fluidized bed and packed bed; hence, the RK only increased in the first 2 weeks, which accounted for the RK increase in the first two weeks, and the reduction in the final two weeks. Further improvements in RK production with an FBR system may be achieved with dynamic management of the gas/liquid flowrate to avoid pellet settlement as well as pellet wash out, thereby achieving stable fluidization. It is quite possible that this system can perform much better in more suitable operating conditions, and may potentially surpass the limitations of other systems by contributing significantly more oxygen and mixing, while avoiding pellet disruption (leading to elutriation/fungal agglomeration).

4. Conclusions

This study comprehensively investigates the effects of agitation and aeration in different bioreactors on pellet morphology and the production of raspberry ketone and raspberry alcohol. Specifically, the PBR resulted in larger, floccose pellets accompanied by maximum titres of 20.6 mg/L RK and 50.9 mg/L RC. STR with impeller mixing yielded compact elliptical pellets, which induced the highest volumetric productivity of 2.0 mg L⁻¹ day⁻¹ and RK selectivity of 0.45. Conversely, the collapsed bed of the FBR led to an RK concentration

of 7.4 mg/L, which was surprisingly 45.6% lower than that in the flask, with a reduction in volumetric productivity of 46%. Based on the study of different bioreactor systems presented here, clear links have been established between bioreactor design, fungal pellet morphology and resultant raspberry ketone production, showing overall that bioreactor design is fundamental in and essential for effective fungal fermentation. Thus, this paper highlights the various bioreactor designs available for fungal fermentation and subsequent bioproduction, and provides a basis for studying industrial sustainability.

Supplementary Materials: The following supporting information can be downloaded at: <https://www.mdpi.com/article/10.3390/fermentation9060546/s1>, Table S1: Phenylalanine concentration during fungal fermentation in different reactors; Table S2: Glucose consumption versus fermentation time in different reactors; Figure S1: Formation mechanism of raspberry ketone and alcohol with the precursor of phenylalanine in fungal fermentation (Zorn et al., 2003) [36]; Figure S2: Fluidization regimes showing the change in pellet fluidization over 4 weeks of fermentation, with a gas flowrate of 0.15 v.v.m.

Author Contributions: Y.Z.: Conceptualization; methodology; data curation; writing—original manuscript. E.C.P.: Methodology; validation; formal analysis; writing—review and editing. Y.L.N.: Conceptualization; validation; writing—review and editing. K.-L.G.: Visualization; data curation; formal analysis. V.Z.: Supervision; writing—review and editing; funding acquisition. Y.C.: Resources; writing—review and editing; supervision; project administration; funding acquisition. All authors have read and agreed to the published version of the manuscript.

Funding: This work was financially supported by Central Public Interest Scientific Institution Basal Research Fund (No. 1610172022014), Newcastle University (LOC/150025720/400382711), and SIFBI (under IAFPP3-H20H6a0028) of A*star, Singapore.

Institutional Review Board Statement: Not applicable.

Informed Consent Statement: Not applicable.

Data Availability Statement: The data that support the findings of this study are available from the corresponding author upon reasonable request.

Conflicts of Interest: The authors have no relevant financial or non-financial interest to disclose.

References

1. Amanullah, A.; Christensen, L.H.; Hansen, K.; Nienow, A.W.; Thomas, C.R. Dependence of morphology on agitation intensity in fed-batch cultures of *Aspergillus oryzae* and its implications for recombinant protein production. *Biotechnol. Bioeng.* **2002**, *77*, 815–826. [CrossRef] [PubMed]
2. Böker, A.; Fischer, M.; Berger, R.G. Raspberry Ketone from Submerged Cultured Cells of the Basidiomycete *Nidula niveo-tomentosa*. *Biotechnol. Prog.* **2001**, *17*, 568–572. [CrossRef]
3. Barros, A.R.; Cavalcante de Amorim, E.L.; Reis, C.M.; Shida, G.M.; Silva, E.L. Biohydrogen production in anaerobic fluidized bed reactors: Effect of support material and hydraulic retention time. *Int. J. Hydrogen Energy* **2010**, *35*, 3379–3388. [CrossRef]
4. Beekwilder, J.; van der Meer, I.M.; Sibbesen, O.; Broekgaarden, M.; Qvist, I.; Mikkelsen, J.D.; Hall, R.D. Microbial production of natural raspberry ketone. *Biotechnol. J.* **2007**, *2*, 1270–1279. [CrossRef]
5. Chen, J.; Zhang, Y.; Zhong, H.; Zhu, H.; Wang, H.; Goh, K.-L.; Zhang, J.; Zheng, M. Efficient and sustainable preparation of cinnamic acid flavor esters by immobilized lipase microarray. *LWT* **2023**, *173*, 114322. [CrossRef]
6. Cui, Y.Q.; van der Lans, R.G.J.M.; Luyben, K.C.A.M. Effect of agitation intensities on fungal morphology of submerged fermentation. *Biotechnol. Bioeng.* **1997**, *55*, 715–726. [CrossRef]
7. dos Reis, C.M.; Silva, E.L. Effect of upflow velocity and hydraulic retention time in anaerobic fluidized-bed reactors used for hydrogen production. *Chem. Eng. J.* **2011**, *172*, 28–36. [CrossRef]
8. Hakkinen, S.T.; Seppanen-Laakso, T.; Oksman-Caldentey, K.M.; Rischer, H. Bioconversion to Raspberry Ketone is Achieved by Several Non-related Plant Cell Cultures. *Front. Plant Sci.* **2015**, *6*, 1035. [CrossRef]
9. Hamrouni, R.; Dupuy, N.; Karachurina, A.; Mitropoulou, G.; Kourkoutas, Y.; Molinet, J.; Maiga, Y.; Roussos, S. Biotechnological potential of Zymotis-2 bioreactor for the cultivation of filamentous fungi. *Biotechnol. J.* **2022**, *17*, e2100288. [CrossRef]
10. Hernandez-Neuta, I.; Pereiro, I.; Ahlford, A.; Ferraro, D.; Zhang, Q.; Viovy, J.L.; Descroix, S.; Nilsson, M. Microfluidic magnetic fluidized bed for DNA analysis in continuous flow mode. *Biosens. Bioelectron.* **2017**, *102*, 531–539. [CrossRef]
11. Kim, S.W.; Hwang, H.J.; Xu, C.P.; Choi, J.W.; Yun, J.W. Effect of aeration and agitation on the production of mycelial biomass and exopolysaccharides in an entomopathogenic fungus *Paecilomyces sinclairii*. *Lett. Appl. Microbiol.* **2003**, *36*, 321–326. [CrossRef]

12. Kowalczyk, M.; Waldron, K.; Kresnowati, P.; Danquah, M.K. Process challenges relating to hematopoietic stem cell cultivation in bioreactors. *J. Ind. Microbiol. Biotechnol.* **2011**, *38*, 761–767. [[CrossRef](#)]
13. Krull, R.; Cordes, C.; Horn, H.; Kampen, I.; Kwade, A.; Neu, T.R.; Nörtemann, B. Morphology of Filamentous Fungi: Linking Cellular Biology to Process Engineering Using *Aspergillus niger*. In *Biosystems Engineering II: Linking Cellular Networks and Bioprocesses*; Wittmann, C., Krull, R., Eds.; Springer: Berlin/Heidelberg, Germany, 2010; pp. 1–21.
14. Li, S.; Li, F.; Zhu, X.; Liao, Q.; Chang, J.S.; Ho, S.H. Biohydrogen production from microalgae for environmental sustainability. *Chemosphere* **2022**, *291*, 132717. [[CrossRef](#)] [[PubMed](#)]
15. Li, X.; Wei, T.; Wu, M.; Chen, F.; Zhang, P.; Deng, Z.Y.; Luo, T. Potential metabolic activities of raspberry ketone. *J. Food Biochem.* **2022**, *46*, e14018. [[CrossRef](#)] [[PubMed](#)]
16. Liang, Z.; Fang, Z.; Pai, A.; Luo, J.; Gan, R.; Gao, Y.; Lu, J.; Zhang, P. Glycosidically bound aroma precursors in fruits: A comprehensive review. *Crit. Rev. Food Sci. Nutr.* **2022**, *62*, 215–243. [[CrossRef](#)] [[PubMed](#)]
17. Liu, E.; Wilkins, M.R. Process optimization and scale-up production of fungal aryl alcohol oxidase from genetically modified *Aspergillus nidulans* in stirred-tank bioreactor. *Bioresour. Technol.* **2020**, *315*, 123792. [[CrossRef](#)]
18. Moore, S.J.; Hleba, Y.B.; Bischoff, S.; Bell, D.; Polizzi, K.M.; Freemont, P.S. Refactoring of a synthetic raspberry ketone pathway with EcoFlex. *Microb. Cell Fact.* **2021**, *20*, 116. [[CrossRef](#)]
19. Moreira, M.T.; Sanromán, A.; Feijoo, G.; Lema, J.M. Control of pellet morphology of filamentous fungi in fluidized bed bioreactors by means of a pulsing flow. Application to *Aspergillus niger* and *Phanerochaete chrysosporium*. *Enzym. Microb. Technol.* **1996**, *19*, 261–266. [[CrossRef](#)]
20. Osadolor, O.A.; Jabbari, M.; Nair, R.B.; Lennartsson, P.R.; Taherzadeh, M.J. Effect of media rheology and bioreactor hydrodynamics on filamentous fungi fermentation of lignocellulosic and starch-based substrates under pseudoplastic flow conditions. *Bioresour. Technol.* **2018**, *263*, 250–257. [[CrossRef](#)]
21. Papoutsakis, E.T. Fluid-mechanical damage of animal cells in bioreactors. *Trends Biotechnol.* **1991**, *9*, 427–437. [[CrossRef](#)]
22. Park, J.P.; Kim, Y.M.; Kim, S.W.; Hwang, H.J.; Cho, Y.J.; Lee, Y.S.; Song, C.H.; Yun, J.W. Effect of aeration rate on the mycelial morphology and exo-biopolymer production in *Cordyceps militaris*. *Process Biochem.* **2002**, *37*, 1257–1262. [[CrossRef](#)]
23. Pereiro, I.; Bendali, A.; Tabnaoui, S.; Alexandre, L.; Srbova, J.; Bilkova, Z.; Deegan, S.; Joshi, L.; Viovy, J.L.; Malaquin, L.; et al. A new microfluidic approach for the one-step capture, amplification and label-free quantification of bacteria from raw samples. *Chem. Sci.* **2017**, *8*, 1329–1336. [[CrossRef](#)]
24. Pereiro, I.; Tabnaoui, S.; Fermigier, M.; du Roure, O.; Descroix, S.; Viovy, J.L.; Malaquin, L. Magnetic fluidized bed for solid phase extraction in microfluidic systems. *Lab Chip* **2017**, *17*, 1603–1615. [[CrossRef](#)]
25. Pleissner, D.; Kwan, T.H.; Lin, C.S. Fungal hydrolysis in submerged fermentation for food waste treatment and fermentation feedstock preparation. *Bioresour. Technol.* **2014**, *158*, 48–54. [[CrossRef](#)] [[PubMed](#)]
26. Rodríguez Porcel, E.M.; Casas López, J.L.; Sánchez Pérez, J.A.; Fernández Sevilla, J.M.; Chisti, Y. Effects of pellet morphology on broth rheology in fermentations of *Aspergillus terreus*. *Biochem. Eng. J.* **2005**, *26*, 139–144. [[CrossRef](#)]
27. Schneider, C.A.; Rasband, W.S.; Eliceiri, K.W. NIH Image to ImageJ: 25 years of image analysis. *Nat. Methods* **2012**, *9*, 671–675. [[CrossRef](#)] [[PubMed](#)]
28. SundarRajan, P.; Gopinath, K.P.; Greetham, D.; Antonysamy, A.J. A review on cleaner production of biofuel feedstock from integrated CO₂ sequestration and wastewater treatment system. *J. Clean. Prod.* **2019**, *210*, 445–458. [[CrossRef](#)]
29. Tan, N.; Ong, L.; Shukal, S.; Chen, X.; Zhang, C. High-Yield Biosynthesis of *trans*-Nerolidol from Sugar and Glycerol. *J. Agric. Food Chem.* **2023**. [[CrossRef](#)]
30. Taupp, D.E.; Nimitz, M.; Berger, R.G.; Zorn, H. Stress response of *Nidula niveo-tomentosa* to UV-A light. *Mycologia* **2008**, *100*, 529–538. [[CrossRef](#)]
31. Taymaz-Nikerel, H.; de Mey, M.; Ras, C.; ten Pierick, A.; Seifar, R.M.; van Dam, J.C.; Heijnen, J.J.; van Gulik, W.M. Development and application of a differential method for reliable metabolome analysis in *Escherichia coli*. *Anal. Biochem.* **2009**, *386*, 9–19. [[CrossRef](#)]
32. Xu, L.; Zhang, Y.; Zivkovic, V.; Zheng, M. Deacidification of high-acid rice bran oil by the tandem continuous-flow enzymatic reactors. *Food Chem.* **2022**, *393*, 133440. [[CrossRef](#)]
33. Zhang, J.; Zhang, J. The filamentous fungal pellet and forces driving its formation. *Crit. Rev. Biotechnol.* **2016**, *36*, 1066–1077. [[CrossRef](#)] [[PubMed](#)]
34. Zhang, Y.; Goh, K.-L.; Ng, Y.L.; Chow, Y.; Wang, S.; Zivkovic, V. Process intensification in micro-fluidized bed systems: A review. *Chem. Eng. Process.* **2021**, *164*, 108397. [[CrossRef](#)]
35. Zhang, Y.; Ng, Y.L.; Goh, K.-L.; Chow, Y.; Wang, S.; Zivkovic, V. Fluidization of fungal pellets in a 3D-printed micro-fluidized bed. *Chem. Eng. Sci.* **2021**, *236*, 116466. [[CrossRef](#)]
36. Zorn, H.; Fischer-Zorn, M.; Berger, R.G. A labeling study to elucidate the biosynthesis of 4-(4-hydroxyphenyl)-butan-2-one (raspberry ketone) by *Nidula niveo-tomentosa*. *Appl. Environ. Microbiol.* **2003**, *69*, 367–372. [[CrossRef](#)] [[PubMed](#)]

Disclaimer/Publisher’s Note: The statements, opinions and data contained in all publications are solely those of the individual author(s) and contributor(s) and not of MDPI and/or the editor(s). MDPI and/or the editor(s) disclaim responsibility for any injury to people or property resulting from any ideas, methods, instructions or products referred to in the content.